Effects of 3-D Printed Structural Characteristics on Magnetic Properties

Lindsey M. Bollig[1], Michael V. Patton[1], Greg S. Mowry[2], and Brittany B. Nelson-Cheeseman[1]

[1]Department of Mechanical Engineering, University of St. Thomas, St. Paul, MN 55105 USA
[2]Department of Electrical Engineering, University of St. Thomas, St. Paul, MN 55105 USA

Additive manufacturing, particularly 3-D printing, allows for completely customizable designs with relatively no limits on geometric complexities. In order to ensure optimal part design for potential magnetic applications, it is crucial to study how the different 3-D printer settings impact the magnetic properties of the printed part. Specifically, in this paper, it was determined how three structural print parameters (outer shell thickness, internal fill factor, and internal layer orientation) affect the resulting magnetic properties of 3-D printed cubic samples. The samples are made using fused deposition modeling of an iron–polymer composite filament. Hysteresis loops were gathered for fields applied along the [100], [110], and [001] directions of the printed cubes. From this, it was determined which combination of print settings should be used to achieve the most desirable magnetic response in terms of magnetic susceptibility, net magnetic moment, and mass-normalized saturation magnetization.

Index Terms— **Additive manufacturing, magnetic anisotropy, magnetic composite materials, soft magnetic materials.**

I. Introduction

ADDITIVE manufacturing, commonly referred to as 3-D printing, refers to the process of building up a part with a material, layer by layer. This allows for the manufacture of complex 3-D geometries without being limited by costly manufacturing steps. One of the most common types of 3-D printing is fused deposition modeling (FDM) [1]. FDM involves heating a thermoplastic polymer in a nozzle and continuously extruding the viscous material onto a print bed to build up a layered 3-D structure. When one layer of the part is complete, the printer head moves up a fraction of a millimeter, so a subsequent layer can be extruded and deposited. This process is repeated until each layer of the part has been extruded and a final 3-D object has been created [2].

While additive manufacturing has seen a surge in interest recently, there has only been limited study of magnetic objects constructed via these layered printing techniques. Micro-stereolithography has been used to create 3-D micro-actuators with complex shapes [3], [4]. 3-D printing of permanent magnets has demonstrated that complex shapes for designer magnetic field profiles can be cheaply achieved [5], [6]. Printing of soft magnetic materials for transformer applications has begun to be explored [7], [8]. Custom electromagnetic interference shielding created by 3-D printing has also been proposed [9].

An important implication of the easily modified nature of a 3-D printed design is that different structural features must be explicitly specified in the printing of a part. First, an outer layer (or *shell*) is almost always used to encase the printed part in a continuous surface that traces the outer perimeter of the part. This shell can range from a single layer to many layers in thickness. Next, the internal *fill factor* is the density or concentration of the extruded lines within the interior of the part; this can be manipulated from 100% to 0% fill. Finally, the internal *fill pattern* constitutes the geometrical pattern of the printed interior of each layer. While there are a variety of fill patterns used, the most common are rectilinear (for its simplicity) and honeycomb (for its structural robustness).

It is widely recognized that the particular selection of each of these print features can influence the properties of the final printed part. This has been most extensively studied in relation to mechanical properties [10], [11]. For printed magnetic parts, these features clearly create structural anisotropies within the printed parts, which have potential implications on the magnetic properties. In particular, the magnetic anisotropy of a part could be modified based on the structural print characteristics chosen. For instance, while not at all expected, could the saturation magnetization of a part be unwittingly changed merely by changing which structural characteristics are selected? Many of these structural factors inherent to 3-D printed objects have not yet been systematically explored to understand how they may affect the magnetic properties of a printed part.

In addition to the large changes in mesoscopic structure made possible by 3-D printing a part, the magnetic properties of magnetic polymer composites can be highly modified by the specific characteristics of the dispersed magnetic phase within the polymer matrix. These factors include particulate material type, size, and shape, as well as collective particulate dispersion, phase fraction, and relative particle alignment. While not the focus of this paper, these factors play a key role in the magnetic properties of any magnetic polymer composite, and may inadvertently be affected by processing and structural factors not explicitly specified and controlled.

Here, we investigate the effects of common 3-D printed structural features on the magnetic properties of the final printed object constructed from a magnetic thermoplastic composite. We find that the layering imposes a rather small,

Manuscript received March 9, 2017; revised April 12, 2017; accepted April 16, 2017. Date of publication April 25, 2017; date of current version October 24, 2017. Corresponding author: B. B. Nelson-Cheeseman (e-mail: bbnelsonchee@stthomas.edu).

Color versions of one or more of the figures in this paper are available online at http://ieeexplore.ieee.org.

Digital Object Identifier 10.1109/TMAG.2017.2698034

0018-9464 © 2017 IEEE. Personal use is permitted, but republication/redistribution requires IEEE permission.
See http://www.ieee.org/publications_standards/publications/rights/index.html for more information.

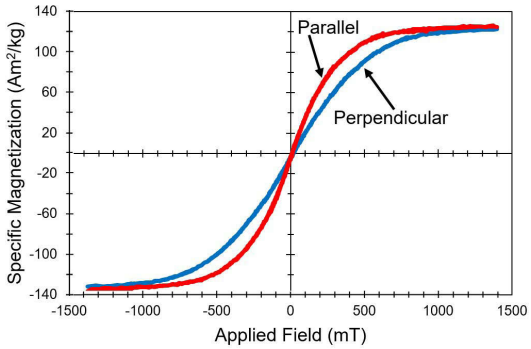

Fig. 1. Magnetic hysteresis loop behavior of 0.5 cm long filament sample before printing for field applied parallel and perpendicular to filament axis. Saturation magnetization is 124 Am^2/kg.

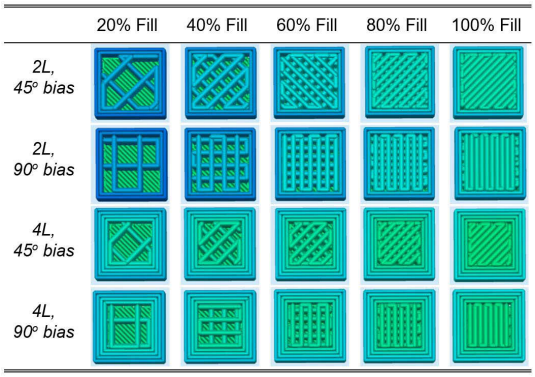

Fig. 2. Diagram of twenty distinct sample architectures. Horizontal cross sections show differences in fill factor, bias of internal layer, and number of outer shell layers.

but noticeable magnetic anisotropy favoring magnetization within the plane of the printed layers versus perpendicular to the printed layers. The orientation of the extruded fill *within* each layer, however, does not yield any significant in-plane anisotropy, resulting in a general magnetic isotropy within the printed layer. Decreasing the shell thickness and fill factor both result in decreased net magnetic moment of the cube, as would be expected. Nevertheless, most importantly, there is a surprising and hitherto unexplained decrease in the mass-normalized magnetization of each cube with increasing fill factor.

II. Methods

A. Filament Characteristics

Samples were created using a commercially extruded magnetic-polymer composite filament from Proto-Pasta (Magnetic Iron PLA). This filament consists of 40 wt.% iron (Fe) particulate embedded in a polylactic acid (PLA) polymer matrix. The PLA matrix is NatureWork's 4043D Ingeo Biopolymer. Previous characterization shows that the iron particles are both inconsistent in size and shape; however, they are roughly isotropic with a diameter of $\sim$40 μm [8]. The magnetic behavior of a 0.5 cm long filament piece (before printing) is shown in Fig. 1.

B. Sample Architectures

Samples were printed as 1 cm^3 cubes with a range of structural print characteristics. The outer shell layer thicknesses were two layers (2L) or four layers (4L). The internal fill factors were 20%, 40%, 60%, 80%, or 100%. It is important to note that these percentages refer to the density of the in-fill lattice within the *interior* of the cubes and *excludes* the outer shell layers. In other words, when specifying the printing of a cube with a given fill factor, the simplify3-D print software does not account for the mass from the outer layers, and only applies fill percentage to the layers making up the internal volume. The outer shell layers are an entirely distinct structural criterion, and it only affects the internal fill in terms of how much volume is left over for the in-fill based on the number of outer shells.

As for fill pattern, due to the unclear structural anisotropy of the honeycomb fill pattern, only the more simplistic rectilinear fill pattern was investigated. However, internal fill orientations of both 45° bias and 90° bias relative to the cube edge were investigated. To clarify, due to the 90° rotation of the in-fill printing orientation for every subsequent layer, the 90° bias samples contain alternating layers aligned 0° and 90° to the cube edge, while the 45° bias samples contain alternating layers aligned 45° and 135° to the cube edge. All possible combinations of these structural print characteristics resulted in 20 unique combinations (or families). Each of these combinations was printed in triplicate, resulting in 60 samples. A diagram illustrating the different cube structures is shown in Fig. 2.

C. Sample Printing

The cubes were created using SolidWorks solid modeling software. The models were then sent to Simplify 3-D software as stereolithography (STL) files, where the software created a g-code of all the commands needed for the custom gCreate thermoplastic 3-D printer to print the samples. The filament extrusion temperature was 212 °C, and an extrusion nozzle width of 0.4 mm was used. A wear resistant nickel-plated brass nozzle was necessary to withstand the abrasion from the iron particulate within the filament as it was extruded.

All of the cubes were printed in the same run in order to ensure that no outside variables, such as humidity or ambient temperature, would differentially affect the printed samples. A printing speed of 3000 mm/min was used for all of the samples. The three nominally identical cubes of each family were printed next to one another, but overall the placement of each family was randomly ordered on the print bed in order to minimize any outside variables with respect to print-bed location or printing time.

In order to minimize the effect of unforeseen process variables, a parallel sequence of printing the cubes was utilized. The sequence of printing proceeded as follows: the first layer of each of the 60 cubes was deposited, with the print head moving randomly between the 60 cubes. Next, the second layer of each of the 60 cubes was deposited, again with the print head moving randomly between the 60 cubes. Then, the third layer of each of the 60 cubes was deposited, and so on, until all of the cubes were completed with the final layer being deposited. In this way, the printing of every one of the cubes progressed in parallel layer-by-layer and was both temporally and spatially randomized within each layer printing as much as possible.

Once printed, each cube was individually marked in order to distinguish each sample from one another. Additionally, an origin was marked on a specific corner of each cubic sample in order to track relative orientation during testing. This marked origin along with the noticeable 3-D printed layering allowed for unambiguous determination of the relative orientation of the [100], [110], and [001] axes.

D. Magnetic Measurements

A Princeton Applied Research vibrating sample magnetometer (VSM) was used to measure hysteresis loops of the samples at room temperature. The samples (1 cm^3) were securely adhered to the vibrating sample holder stick using tape. The sample holder and sample were centered along all three axes between the pick-up coils. Hysteresis loops were collected to +/−1.4 T. No diamagnetic or paramagnetic linear subtractions were made to the data. The mass of each printed cube was measured immediately before being loaded into the VSM to ten thousandths of a gram. The saturation moment was divided by the measured mass to compute the mass-normalized magnetization of each sample.

In order to assess magnetic anisotropy due to the 3-D printed architecture, hysteresis loops were collected with the applied magnetic field oriented along the [100], [110], and [001] directions relative to the cube's marked origin. Note that the magnetic field was oriented parallel to the plane of the printed layers for [100] and [110], and perpendicular to the printed layers for [001].

III. Results

A. General Hysteresis Loop Characteristics

All of the printed cubes exhibited very magnetically soft hysteresis loops with low coercivity (∼25 mT) and clear saturation behavior below 1000 mT (in most cases, below 500 mT). This magnetic behavior is consistent with previously measured magnetic properties of the filament material [8]. Unfortunately, the demagnetization effects from the cube sample geometry [12], as well as the roughly isotropic Fe particulate, lead to saturation at higher fields than would be ideal for soft magnetic applications.

B. Effects of Field Orientation

For a given cube, changing the magnetic field orientation within the plane of the printed layer has little to no change on the magnetic susceptibility or demagnetization behavior exhibited by that cube. As shown in Fig. 3, when comparing the hysteresis loops obtained from the [100] and [110] field orientations, they strongly overlap one another, lying almost directly on top of one another. This holds true for all samples tested.

Nevertheless, there are noticeable changes when the magnetic field is applied perpendicular to the printed layers compared to within the plane of the printed layers of that cube. As shown in Fig. 3, the susceptibility decreases when the magnetic field is applied out of plane along the [001], indicating greater demagnetization effects. This difference was present for all samples.

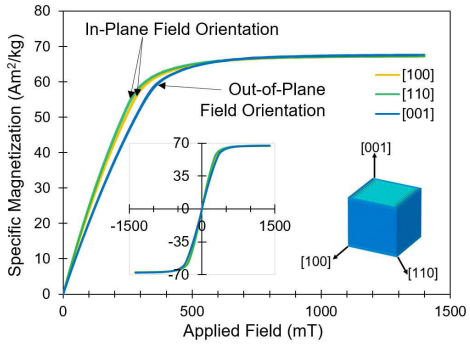

Fig. 3. Hysteresis loops for an applied field along [100], [110], and [001]. Main panel shows zoomed first quadrant of hysteresis loop, while inset shows complete four-quadrant hysteresis loop data. Data shown are from 2L 40% fill samples.

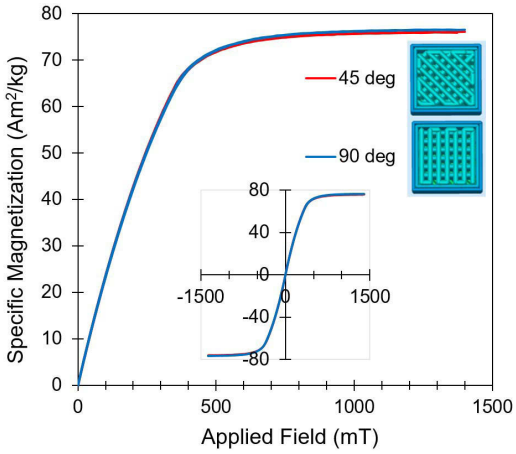

Fig. 4. Hysteresis loops as a function of in-plane fill orientation. Main panel shows zoomed first quadrant of hysteresis loop, while inset shows complete four-quadrant hysteresis loop data. Data shown are from 2L 60% fill samples.

C. Effects of Internal Fill Orientation Within a Layer

As shown in Fig. 4, the orientation of the inner fill (45° bias versus 90° bias) does not significantly affect the magnetic susceptibility or demagnetization of the cubes. The presence of an easy plane parallel to the layering, as opposed to any preferred easy axis within the plane, demonstrates that the printed layers act closer to an oblate spheroid rather than the individual printed lines acting as individual prolate spheroids. Additionally, the rather small size of the anisotropy difference between in-plane and out-of-plane hysteresis loops is likely due to the generally isotropic nature of the Fe particulate within the PLA matrix. Still, an out-of-plane hard axis persists suggesting that the processing of the cube in the layer-by-layer fashion somehow imposes an in-plane magnetic character on the sample. The specific origin of this effect has not been resolved at this time; however, issues related to processing (cooling time, magnetic annealing, flow characteristics, etc.) and the resulting structure (particulate orientation, inter-particle effects, etc.) are all potential factors.

D. Effects of Internal Fill Factor

The effects of internal fill factor were determined by comparing the cubes with 100%, 80%, 60%, 40%, and 20% internal fills and both two outer shell layers [Fig. 5(a)] and four outer shell layers [Fig. 5(b)]. There is a clear trend

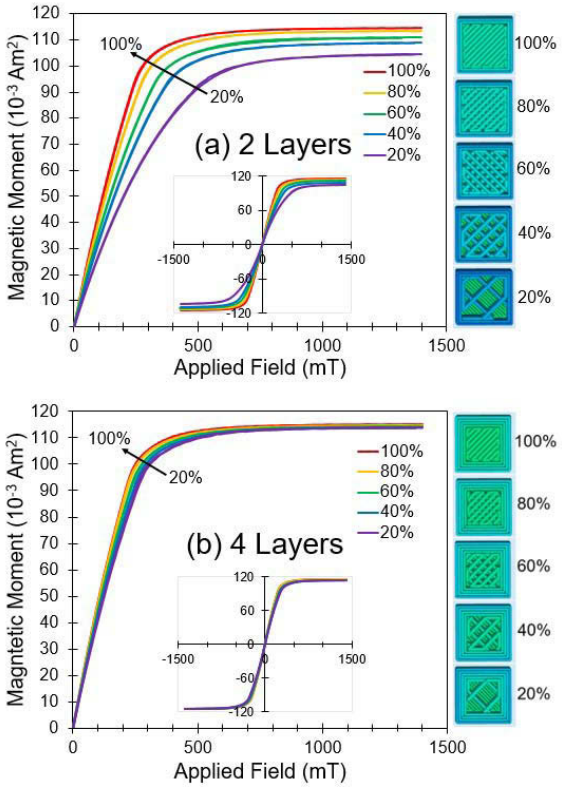

Fig. 5. Effect of fill factor on magnetic moment versus applied field for cubes with (a) 2L, 45° infill layer orientation and (b) 4L, 45° infill layer orientation. Main panels show zoomed first quadrant of hysteresis loop, while insets show complete four-quadrant hysteresis loop data. Right-hand side graphics illustrate cube cross section for each fill % and shell layer thickness.

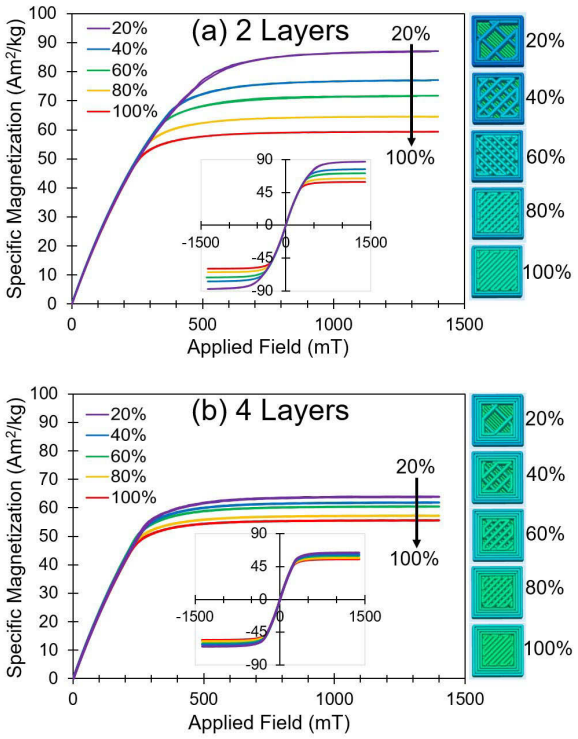

Fig. 6. Effect of fill factor on magnetization versus applied field for cubes with (a) 2L, 45° infill layer orientation and (b) 4L, 45° infill layer orientation.

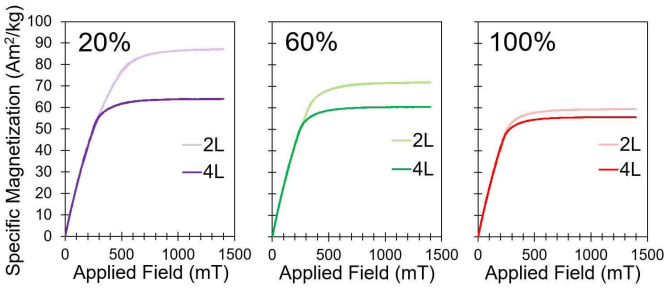

Fig. 7. Magnetization versus applied field hysteresis loops directly comparing the two-shell layer (2L) and four-shell layer (4L) samples for the 20%, 60%, and 100% fill factors. Only first quadrant is shown for clarity.

for the internal fill factor. The cubes with 100% internal fill have the largest magnetic saturation moment, systematically decreasing, with the 20% internal fill cubes having the smallest magnetic saturation moment. This is expected since an internal fill of 100% contains the most material and thus has the most iron. This should result in a larger moment in the applied magnetic field, which is seen.

However, when the moment of each cube is normalized by its own mass to find the magnetization (Am^2/kg), one can see in Fig. 6 that there is an unexpected decrease in the saturation magnetization (MS) with increasing internal fill factor. This is a surprising result. One would expect that the MS of the samples would be nearly identical given the normalization by the mass (nominally, the amount of filament used).

E. Effects of External Shell Layers

The same overall trend of increasing saturation moment for increasing internal fill factor is seen among both the 2L and 4L cubes. However, there is a clear difference in magnitude of this spread (Fig. 5). The 2L samples have a larger spread in the saturation moment between the 100% and 20% internal fill factors than the spread in the 4L cubes. This is likely because more internal volume is taken up by the internal layers when less shell layers are present.

As shown in Fig. 7, when comparing the magnetization hysteresis loops of the 2L and 4L cubes of 100% fill factor, there was only a small difference between the two. Since these samples are both almost completely dense, it makes sense that they would exhibit roughly the same MS. However, as the fill factor is decreased, the difference between the MS(2L) and MS(4L) for a given fill factor becomes even greater. This leads one to reiterate that the source of the enhancement in MS originates most explicitly with the interior fill itself and not with the outer shell.

In order to compare any changes in susceptibility and demagnetization behavior as a function of fill factor, the normalized magnetization behavior of all the fill factors is shown in Fig. 8. Both the 2L and 4L series show lower susceptibility and higher demagnetization effects as the fill factor is decreased. Again, the 2L samples show a greater change with fill factor compared with the 4L samples due to the larger percentage of internal fill volume present.

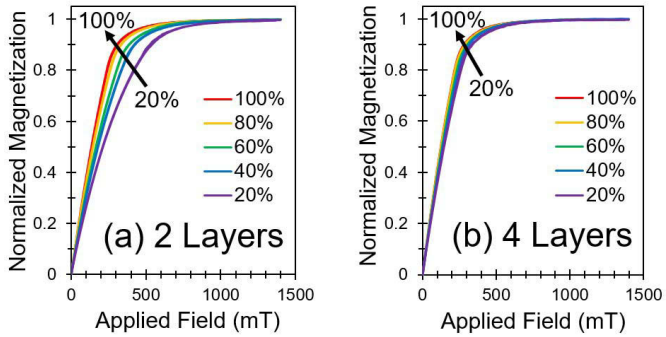

Fig. 8. Normalized magnetization for (a) 2L, 45° infill layer orientation and (b) 4L, 45° infill layer orientation.

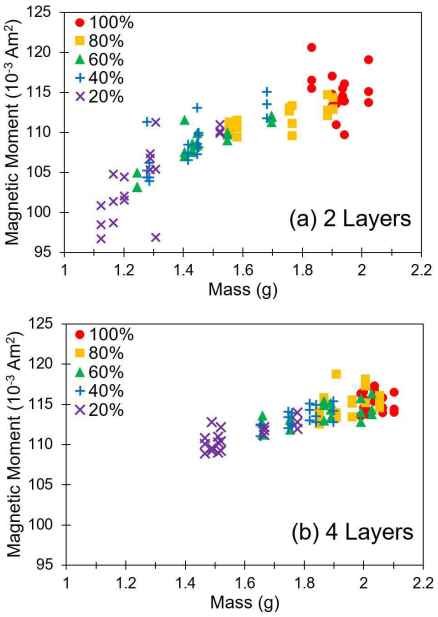

Fig. 9. Saturation moment versus mass for all samples with (a) two shell layers (2L) and (b) four shell layers (4L). Data are categorized by internal fill factor.

IV. Discussion

When anomalies in saturation magnetization data arise, both the saturation moment and mass must be heavily scrutinized. A summary of the saturation moment as a function of sample mass for all samples is shown in Fig. 9. The data are also parsed by internal fill factor. Since each fill factor category (e.g., 20%) had four distinct cube structures (Fig. 2), the masses of each fill factor category cover a range associated with all of those sub-structures. Nevertheless, the trend of decreasing saturation moment with decreasing mass is seen, as expected.

A summary of the M_S as a function of sample mass is shown in Fig. 10. While one expects a given material to exhibit no change in M_S as the total mass of that material changes (i.e., a straight flat line), a linear negatively sloped trend is seen from the data. At this time, the origin of this remains unclear. When compared with the M_S of the pre-printed filament, the data trend appears not to be of anomalously increasing magnetization with decreasing internal fill %, but rather of decreasing magnetization (from the expected composite M_S) with increasing internal fill %. Note that the highest fill

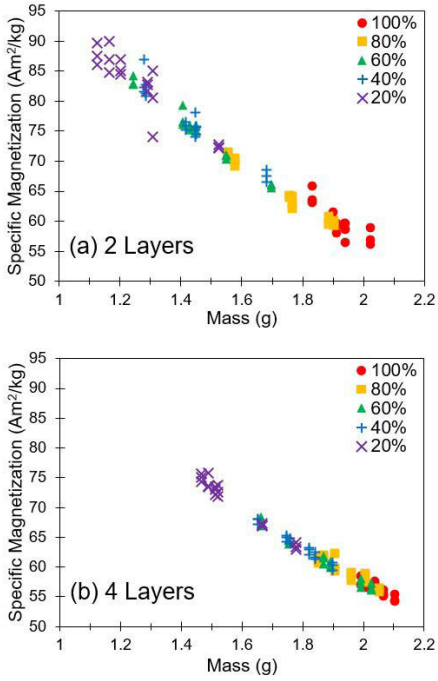

Fig. 10. Saturation magnetization versus mass for all samples with (a) two shell layers (2L) and (b) four shell layers (4L). Data are categorized by internal fill factor.

samples would create the largest moment, and are thus likely most desirable for a number of applications [8]. Thus, it is important that there appears to be a decrease in M_S for these largest internal fill factors.

Conceivably, only by changing the relative content of Fe in the composite filament can one change the magnetization of the printed samples. However, the Fe content is believed to be constant throughout the filament, and, furthermore, the samples were all printed simultaneously in parallel and in a randomized order. This suggests that a change may be occurring to the Fe particulate when fill factor is decreased from 100%–20% internal fill.

An alternative explanation could reside with the PLA matrix, which may comprise a small amount of residual solvents or other volatile admixtures. It is possible that these admixtures more easily vaporize from samples of lower filling factors, while remaining denser in samples of higher fill factors.

Other possibilities include that the sample vibration from the VSM is damped when cubes of higher mass are attached to the sample holder or that the magnetic field from the large samples deviates from ideal point dipoles that the calibration of the magnetometer likely assumes. Future studies will investigate smaller sample sizes and utilize other magnetic measurement methods to see if the pattern is reproduced.

Finally, while not the focus of this paper, one notes a number of factors that could be modified in order to produce samples with softer, more-square hysteresis loops. In particular, the particulate shape and orientation could be optimized. The roughly isotropic particulate imposes a demagnetization effect upon the resulting hysteresis loops. If particulate with one or two elongated axes (approximating prolate spheroids or oblate

spheroids, respectively) could be utilized, the demagnetization effects could be minimized resulting in softer hysteresis loops with higher susceptibilities. Additionally, some mechanism of magnetic annealing during or after printing would likely help create favorable alignment of both the particles and pinned dipoles along a specific desired axis. Macroscopic printing of part shapes approximating more prolate or oblate spheroids may also result in more abrupt switching along easy directions. Indeed, FDM is well-suited to print optimized shapes that may be otherwise prohibitive under normal manufacturing conditions.

V. Conclusion

In conclusion, the magnetic properties of 3-D printed structures were investigated. Cubic samples were made using a commercial iron-PLA composite filament and 3-D printed using a thermoplastic 3-D printer. The influences of internal fill factor, orientation of the inner layers, and number of external shell layers were investigated by studying the resulting magnetic susceptibility, saturation moment, and saturation magnetization. Regardless of printing parameters, the samples display an easy plane coincident with the printed layer orientation, and a hard axis perpendicular to the printed layers. As both the shell layer thickness and internal fill factor increase, the saturation moment increases as expected. Unexpectedly, the mass-normalized magnetization (Am^2/kg) decreases as the internal fill factor increases.

Acknowledgment

Part of this work was performed by LB as a Visiting Fellow at the Institute for Rock Magnetism (IRM) at the University of Minnesota. The IRM is a U.S. National Multi-user Facility supported through the Instrumentation and Facilities Program of the National Science Foundation, Earth Sciences Division, and by funding from the University of Minnesota. This work was supported in part by the Renewable Energy and Alternatives Laboratory at UST and in part by funding through the UST Young Scholar's Grant and UST Grants and Research Office. The authors would like to thank A. Otto for assistance with the 3-D printer and P. Ryan for thoughtful discussions. They would also like to thank B. Stadler and P. Dulal for preliminary VSM measurements.

References

[1] N. Guo and M. C. Leu, "Additive manufacturing: Technology, applications and research needs," *Frontiers Mech. Eng.*, vol. 8, no. 3, pp. 215–243, Sep. 2013, doi: 10.1007/s11465-013-0248-8.

[2] I. Gibson and D. R. B. Stucker, *Additive Manufacturing Technologies*. New York, NY, USA: Springer, 2010.

[3] K. Kobayashi and K. Ikuta, "Three-dimensional magnetic microstructures fabricated by microstereolithography," *Appl. Phys. Lett.*, vol. 92, p. 262505, Jul. 2008.

[4] M. Yasui, M. Ikeuchi, and K. Ikuta, "Density controllable photocurable polymer for three-dimensional magnetic microstructures with neutral buoyancy," *Appl. Phys. Lett.*, vol. 103, p. 201901, Nov. 2013.

[5] C. Huber *et al.*, "3D print of polymer bonded rare-earth magnets, and 3D magnetic field scanning with an end-user 3D printer," *Appl. Phys. Lett.*, vol. 109, p. 162401, Oct. 2016.

[6] L. Li *et al.*, "Big area additive manufacturing of high performance bonded NdFeB magnets," *Sci. Rep.*, vol. 6, Oct. 2016, Art. no. 36212.

[7] Y. Yan, K. D. T. Ngo, Y. Mei, and G.-Q. Lu, "Additive manufacturing of magnetic components for power electronics integration," in *Proc. ICEP*, Apr. 2016, pp. 368–371, doi: 10.1109/ICEP.2016.7486849.

[8] L. M. Bollig, P. J. Hilpisch, G. S. Mowry, and B. B. Nelson-Cheeseman, "3D printed magnetic polymer composite transformers," *J. Magn. Magn. Mater.*, vol. 442, pp. 97–101, Nov. 2017.

[9] M. Nikzad, "New metal/polymer composites for fused deposition modelling applications," Ph.D. dissertation, Faculty Eng. Ind. Sci., Swinburne Univ. Technol., Melbourne, VIC, Australia, 2011.

[10] S.-H. Ahn, M. Montero, D. Odell, S. Roundy, and P. K. Wright, "Anisotropic material properties of fused deposition modeling ABS," *Rapid Prototyping J.*, vol. 8, no. 4, pp. 248–257, Oct. 2002.

[11] H. Rezayat, W. Zhou, A. Siriruk, and D. Penumadu, "Structure–mechanical property relationship in fused deposition modelling," *Mater. Sci. Technol.*, vol. 31, pp. 895–903, Jun. 2015.

[12] A. Aharoni, "Demagnetizing factors for rectangular ferromagnetic prisms," *J. Appl. Phys.*, vol. 83, no. 6, pp. 3432–3434, Jun. 1998.